Trans Indian Inst Met (2015) 68(2):247–255
DOI 10.1007/s12666-014-0452-1

TECHNICAL PAPER

TP 2850

Effect of Welding Time in the Resistance Spot Welded Dissimilar Stainless Steels

Mohammad Hosein Bina · Mostafa Jamali · Morteza Shamanian · Hamed Sabet

Received: 6 November 2013 / Accepted: 2 August 2014 / Published online: 26 October 2014

Abstract In this study, the effect of welding time on joining capability of austenitic stainless steel (AISI 304) sheets and ferritic stainless steel (AISI 430) sheets by using resistance spot welding (RSW) process was investigated. Therefore, macrostructure, microstructure, microhardness, tensile shear strength, and failure mode of welded materials were determined for various welding times. The welding times values used in the resistance spot welding process were 0.4, 0.8, 1.2, and 1.6 s. Tensile shear tests carried out on the welded joints determined their strength and failure mode. The increase in the welding time resulted in an increase in the nugget size and the weld strength. Two distinct failure modes were observed during the tensile shear test: interfacial, pullout failure modes. Finally, an optimum welding time was obtained.

Keywords Welding · Stainless steels · Optical microscopy · Mechanical testing

M. H. Bina (✉)
Department of Advanced Materials and New Energies, Iranian Research Organization for Science and Technology, Tehran, Iran
e-mail: bina@ma.iut.ac.ir

M. Jamali · H. Sabet
Department of Materials Engineering, Islamic Azad University-Karaj Branch, Karaj, Iran

M. Shamanian
Department of Materials Engineering, Isfahan University of Technology, 84156-83111 Isfahan, Iran

1 Introduction

Several situations arise in industrial practice which calls for joining of dissimilar materials. The materials employed are location dependent in the same structure for effective and economical utilization of the special properties of each material. Joining of dissimilar metals is generally more challenging than that of similar metals because of difference in the physical, mechanical and metallurgical properties of the parent metals to be joined. In order to take full advantage of the properties of different metals it is necessary to produce high quality joints between them. Only in this way can the designer use most suitable materials for each part of a given structure. Growing availability of new materials and higher requirements being placed on materials creates a greater need for joints of dissimilar metals [1].

During the last ten years, the usage of stainless steel materials increased continuously in various industrial applications [2, 3] and medical applications [3, 4]. Stainless steel sheets are increasingly used for vessels, kitchen, building, transportation, etc., because of their high corrosion resistivity, beautiful appearance [3, 5, 6] and a reasonable weldability [3, 7]. Dissimilar metal combination between ferritic stainless steels and austenitic stainless steels is commonly employed in TiCl4 reduction retorts. This calls for welding of the combination. Such transition joints are necessary because austenitic stainless steels with superior creep strength and oxidation resistance are required in the higher temperature regions, while ferritic stainless steels are used to avoid the problem of nickel leaching by molten magnesium. Welding of ferritic to austenitic stainless steels is considered to be a major problem due to difference in coefficient of thermal expansion, which may lead to crack formation at the interface, formation of hard zone close to the weld interface, relatively soft regions

Table 1 Chemical composition of AISI 304 austenitic stainless steel and AISI 430 ferritic stainless steel (wt%)

	Fe	Cr	Ni	Mn	C	Si	Nb	S	Mo
AISI 430	Bal.	17.5	0.141	0.769	0.12	0.471	–	0.01	–
AISI 304	Bal.	18.4	8.94	1.49	0.072	0.367	0.148	0.03	0.042

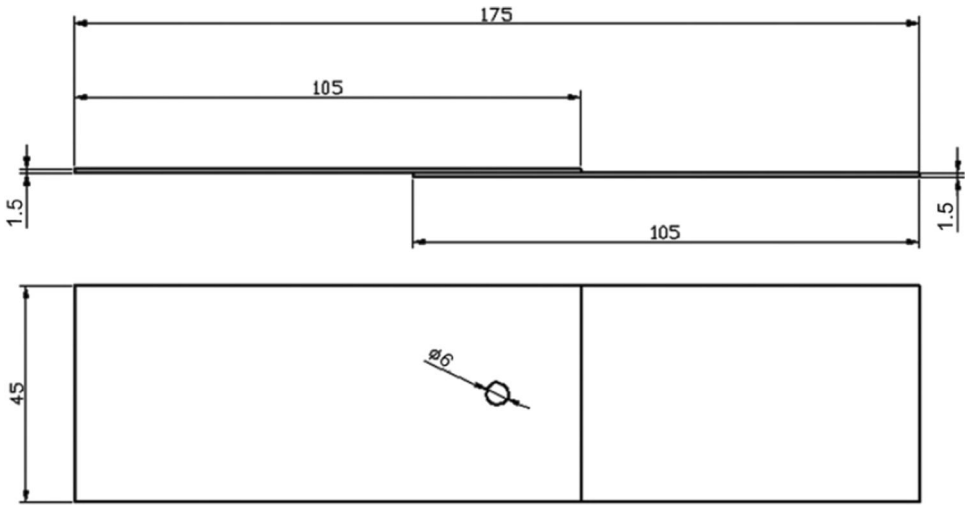

Fig. 1 The sizes of tensile shear test samples

adjacent to the hard zone; large hardness difference between the hard and soft zones and expected differences in microstructure may lead to failures in service [1].

Resistance spot welding (RSW) that is one of the oldest electric welding processes in use by industry today is a joining technique which is used for almost all known metals. The weld is made by a combination of heat, pressure and time [8, 9]. Electrical resistance of the material to be welded causes a localized heating at the interface of the metals to be joined. Because the processes requires relatively simple equipment; it is easily and normally automated and once the welding parameters established it should be possible to produce repeatable welds. Resistance spot weld is the most widely used joining process for sheet materials. The process is used in preference to mechanical fasteners, such as rivets or screws, when disassembly for maintenance is not required [9, 10].

Several works are available in literature regarding the welding processes used to join austenitic stainless steel to ferritic stainless steel, among which are methods such as laser and friction welding processes [1, 11–13]. However, there is no information about dissimilar weld between austenitic stainless steel and ferritic stainless steel by resistance spot welding process. Thus, the aim of this research is to join the austenitic stainless steel to ferritic stainless steel and to investigate the effect of the different welding times on microstructure and mechanical properties of the welded materials.

2 Experimental Procedure

In the present work, austenitic stainless steel sheet (304 grade) and ferritic stainless steel sheet (430 grade) with a thickness of 1.5 mm were used. The chemical composition of austenitic and ferritic stainless steels sheets are shown in Table 1. A timer and current controlled electrical resistance spot welding machine having 30 kVA capacity and pneumatic application mechanism were used in experiments. Welding was carried out by using water cooled conical Cu–Cr electrodes having a contact surface of the same diameter (7 mm). For joining, different welding times were applied (0.4, 0.8, 1.2, and 1.6 s), while other welding parameters such as the weld current (3.75 kA) and electrode pressure were kept constant. The transverse sections of the weld passing through the weld nugget as well as the similar section of the base plates were prepared by standard metallographic procedure. Samples were electro-etched in a solution containing 50 vol% chloride acid.

The welded parts according to ISO 14273 were prepared for tensile shear tests (Fig. 1) in a Hounsfield testing machine in laboratory conditions. The tensile speed was constant during the test (10 mm/min). Values of the tensile shear load were obtained from the load-extension graphs. The microhardness measurements were carried out using a Leitz Wetzlar type Vickers hardness machine under a 100 g load. Measurements on each sample were taken in one direction, along the radius of the nugget (Fig. 2).

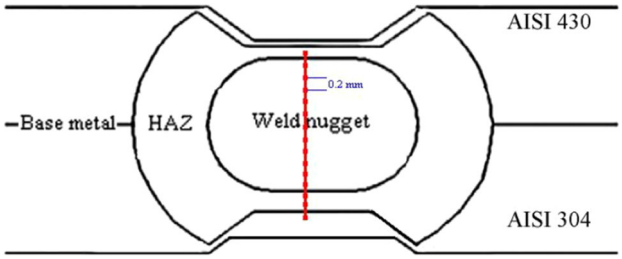

Fig. 2 Microhardness profiles of welded sheets

3 Results and Discussion

3.1 Macrostructural Observations

The most important factors that affect weld quality in the resistance spot welding process are surface appearance, strength and ductility, weld nugget size, weld penetration, sheet separation, and internal discontinuities [3, 14, 15]. Surface appearance of the welded dissimilar materials is shown in Fig. 3. Normally, the surface appearance of a spot weld should be relatively smooth, round or oval in the case of contoured work and free from surface fusion, electrode deposits pits, cracks and deep electrode indentation [3, 14, 15]. In the present work, the smooth weld surface appearance was obtained in almost all welded materials except the sample with maximum welding time (1.6 s). The electrode deposits pits were observed on some of the welded materials. The electrode indentation was found acceptable for all welded materials except 1.6 s. It may be attributed to the proper and uniform electrode pressure. The electrode force affects the appearance of the resistance spot weld. For sample with maximum welding time (1.6 s), the overheating between the electrodes and the samples caused surface flashing, picking up metal on the electrode, and poor surface appearance.

The macrostructures of dissimilar resistance spot weld between austenitic stainless steel and ferritic stainless steel at various welding times are shown in Fig. 4. As can be seen, the joint region consists of three distinct structural zones, namely [16, 17]:

1. Weld nugget (WN) which is melted during the welding process and is resolidified showing a cast structure. Macrostructure of the WN consists of columnar grains.
2. Heat affected zone (HAZ) which is not melted but undergoes microstructural changes.
3. Base metal (BM).

As is a known fact that the heat input in the resistance spot welded joints increases with the increase in the welding time. The amount of heat generated depends on three factors: (1) the weld current, (2) the resistance of the materials, and (3) the welding time. In this study, the weld current was constant (3.75 kA) as well as the resistance of parent materials. Therefore, welding time is effective on the heat input and the weld nugget diameter. Figure 4 illustrates that the increase in the welding time results in an increase in the nugget diameter on both the austenitic and ferritic stainless steel sides.

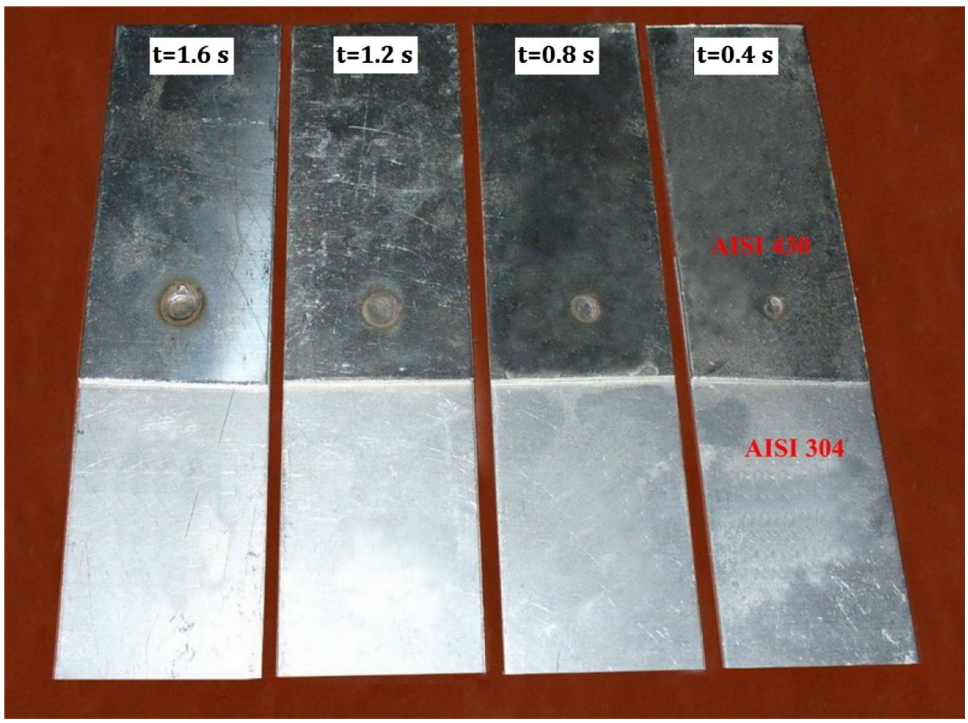

Fig. 3 Macrographs of the resistance spot welded materials with various welding times

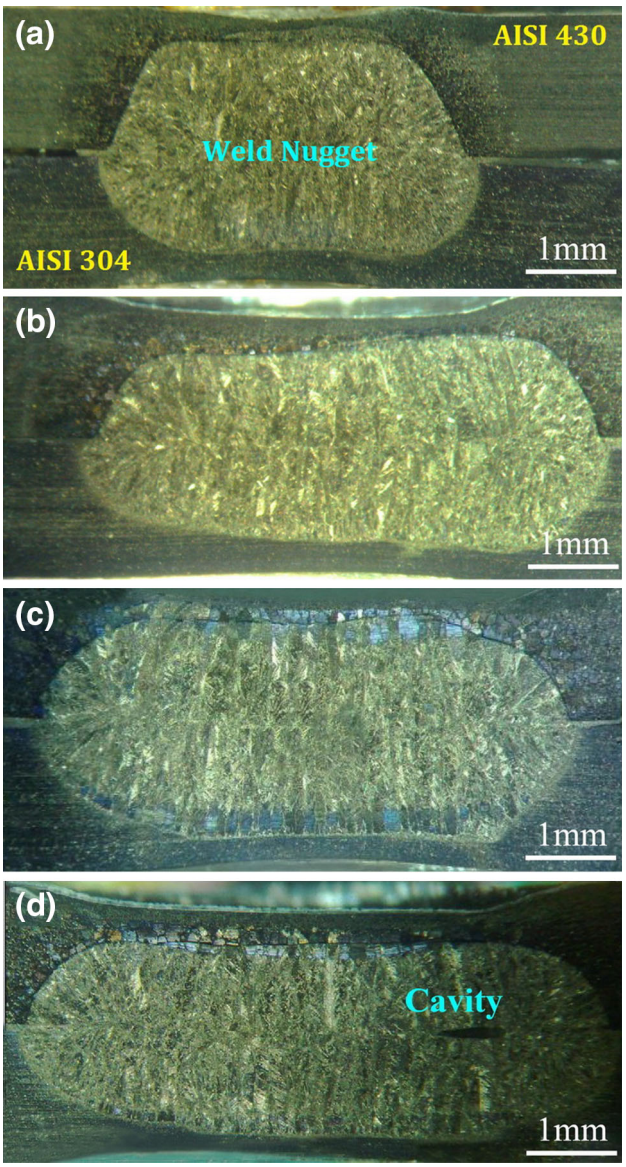

Fig. 4 Macrostructure of dissimilar resistance spot welded between austenitic and ferritic stainless steels for various welding times: **a** 0.4, **b** 0.8, **c** 1.2, and **d** 1.6 s

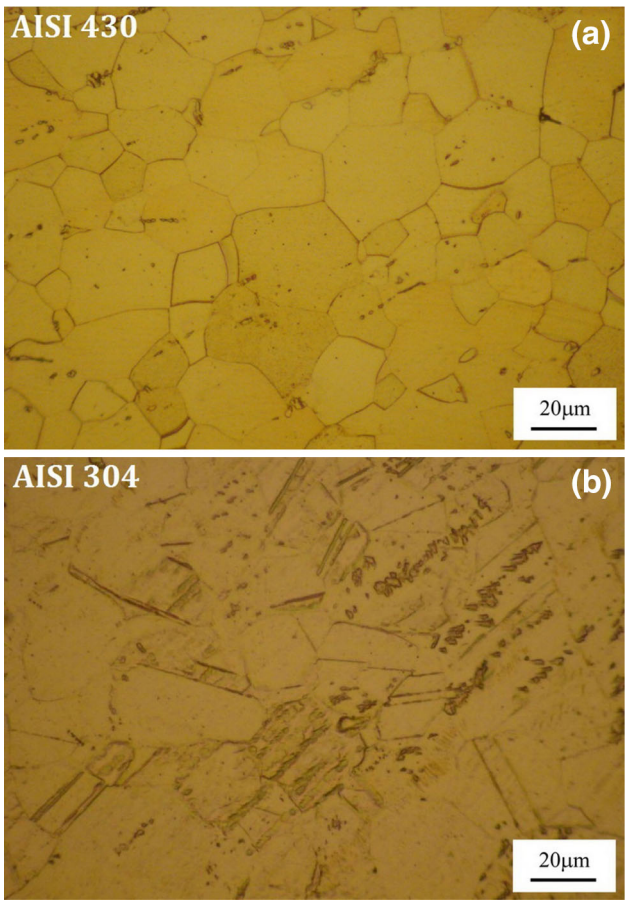

Fig. 5 Optical microstructure of parent materials: **a** ferritic stainless steel (AISI 430) and **b** austenitic stainless steel (AISI 304)

One of the important features of weld nugget is its asymmetrical shape such that the weld nugget size (diameter) of austenitic stainless steel (AISI 304) side were larger than that of ferritic stainless steel (AISI 430) side. Electrical resistance and thermal conductance control heat generation and heat dissipation which in turn, affect weld nugget formation and its growth [15–17]. Differences in the thermal conductivity and electrical resistivity of two steel sheets lead to an asymmetrical weld nugget in dissimilar metal joints. Also, electrical resistance of the AISI 430 is lower than that of the AISI 304. This leads to smaller WN diameter in the ferritic stainless steel. In fact, the weld nugget lost its symmetric form due to the unbalanced heat resulting from different physical properties of the steel sheets. However, selection of the suitable time (1.2 s) led to a symmetrical WN region in the joint.

Weld penetration is the depth to which the nugget extends into the pieces that are in contact with the electrodes. Minimum depth of penetration is generally accepted as 20 % of the thickness while the depth of penetration should not exceed 80 % of the thickness [9, 14, 15]. The penetration was found between 20 and 80 % of the thickness of the base metals for all welding times. It should be noted that the HAZ and penetration depth of weld nugget in the ferritic stainless steel side were larger than those in the austenitic stainless steel side, which can be related to higher thermal conductivity of AISI 430 sheet. Also, the ferritic stainless steel side of welded materials was observed deeper electrode indentation rather than austenitic stainless steel side due to low yield strength of AISI 430 sheet.

Internal discontinuities include cracks, porosity or spongy metal, large cavities and metallic inclusions [3, 9,

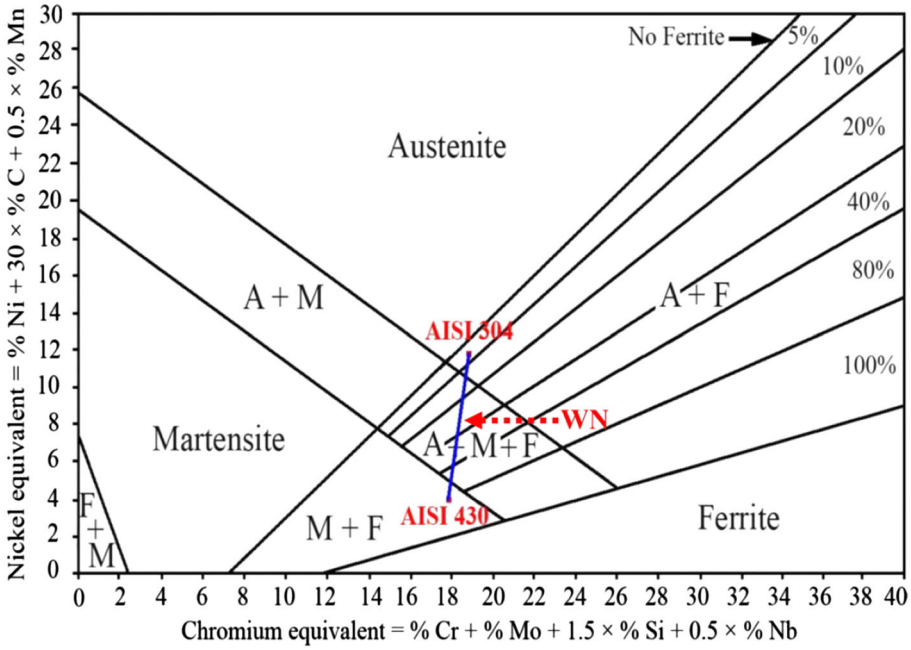

Fig. 6 Schaeffler diagram, weld nugget microstructure prediction, when dilution is 50 %

14, 15, 18]. Cavity was observed in sample with maximum welding time. A cavity occupied in the centre of the weld nugget is shown in Fig. 4d. These internal defects in spot weld are generally caused by high welding time, low electrode force, high weld current or any other conditions that produce excessive weld heat [3, 9, 15, 19]. Due to high thermal expansion, high welding shrinkage strains can be responsible for these internal defects.

3.2 Microstructural Observations

The parent materials employed in the present work were AISI 304 austenitic stainless steel and AISI 430 ferritic stainless steel. As can be seen in Fig. 5, the ferritic stainless steel consisted of coarse and elongated grains of ferrite, while the austenitic stainless steel contained equiaxed grains of austenite with occasional twinning.

Microstructure of the weld nugget of dissimilar metal joint between austenitic stainless steel and ferritic stainless steel can be predicted using constitution diagrams, e.g., Schaeffler diagram [14]. It should be noted that the application of Schaeffler diagram might be inaccurate due to very high cooling rates of resistance spot welding process [17]. As can be seen in Fig. 6, when dilution is 50 %, the predicted microstructure of the weld nugget of a dissimilar metal joint between austenitic and ferritic stainless steels is martensite + austenite + ferrite (δ). In this study, the values of dilution were 50–70 %. However, it is important that changing the welding time from 0.4 to 1.6 s which led to changing the dilution value, had no effect on predicted microstructure of the weld nugget.

The microstructure of samples that were welded in various welding times are shown in Figs. 7 and 8. These figures indicate that the microstructure of welded samples is in agreement with the predicted weld nugget microstructure using the Schaeffler diagram. Martensite formation in the weld nugget is attributed to high cooling rate of resistance spot welding process due to the presence of water cooled copper electrodes and their quenching effect as well as short welding cycle. From Figs. 7 and 8, the weld nugget had a columnar structure and the grains of WN zone were elongated parallel to the electrode compression direction. It was found that the grain size of weld nugget and HAZ were increased by increasing the welding time. The microstructures of these areas were considerably different from that of original base metal. Unlike the base metal, it is noted that grain growth occurred due to the heat transfer. The area of HAZ was found wider on ferritic stainless steel side that have higher thermal coefficient than austenitic stainless steel. In the austenitic stainless steel, the austenitic matrix shows relatively low alloying element diffusion rates, a high thermal expansion coefficient and high electric resistance. Therefore, when compared with ferritic stainless steel, grain growth and solid state transformation in the HAZ tend to occur slowly, but welding shrinkage strains can be very high [15]. The microstructure of weld nugget is mixture of austenite, ferrite and martensite and there is solid state transformation. With increase in welding time, heat input increases and this results in increase in nugget size; not change in the relative volume fractions of various phases in the weld nugget zone. This could be the reason for not observing significant

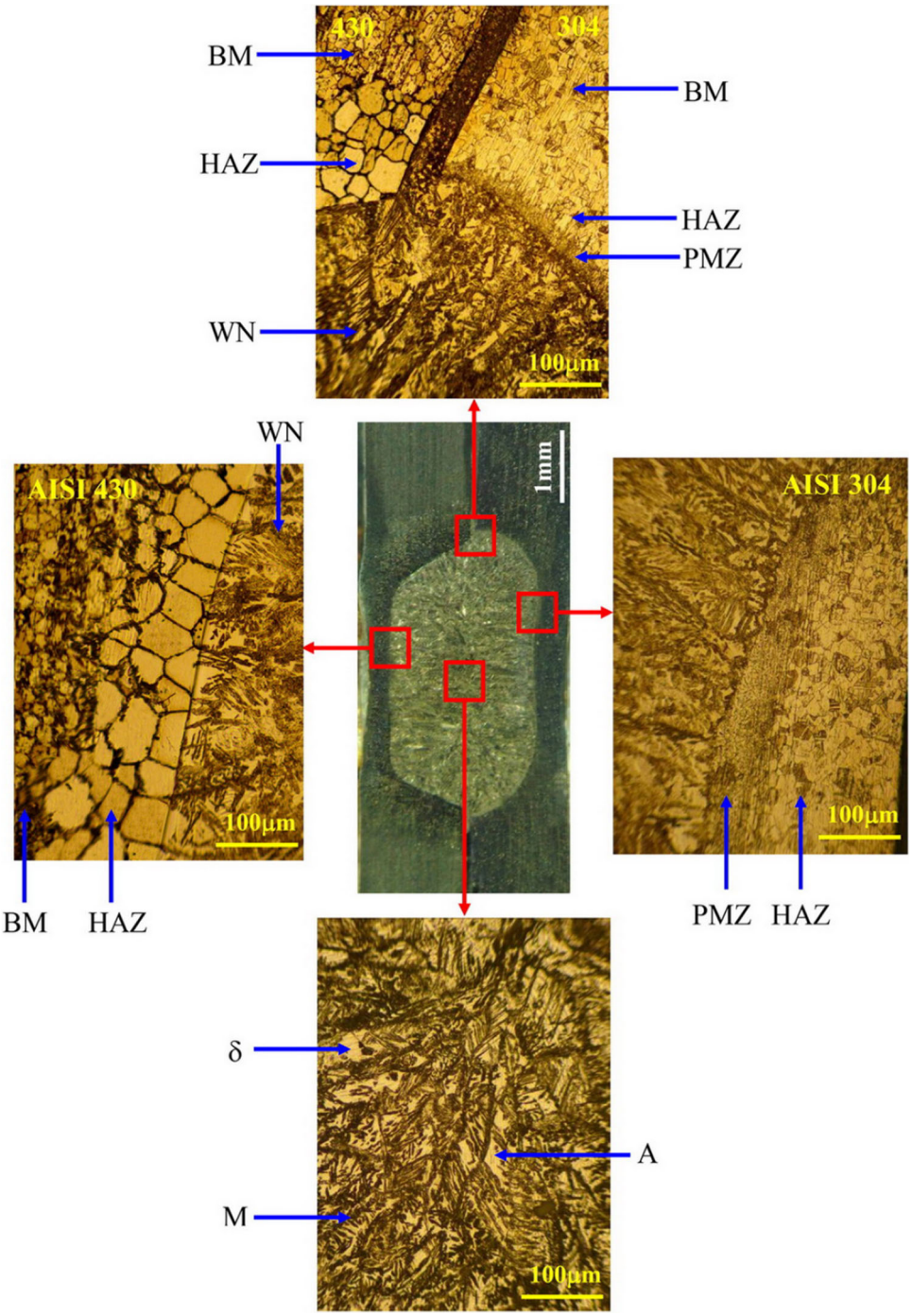

Fig. 7 Microstructure of resistance spot welded sample with 0.4 s welding time

change in the microstructure of the nugget zone with increase in welding time. Further, there is no transformation during weld thermal cycling in ferritic stainless steel 430 also. This is clear from the coarse ferritic grains of the HAZ of this steel.

3.3 Mechanical Properties

The microhardness measurement was performed on the weld nugget, heat affected zone, and base metals of sample as seen in Fig. 9. The microhardness distributions for the four various welding times of the joints were almost same. Therefore, one of them (1.2 s) showed (Fig. 9). As seen in Fig. 9, the hardness of WN was found to be higher than that of the HAZ and BM. It was observed that the maximum hardness value is in the middle of the weld nugget. The highest hardness value of the joint was approximately 360 HV.

It was mentioned that the hardness values of joints did not show any considerable fluctuation for either welding

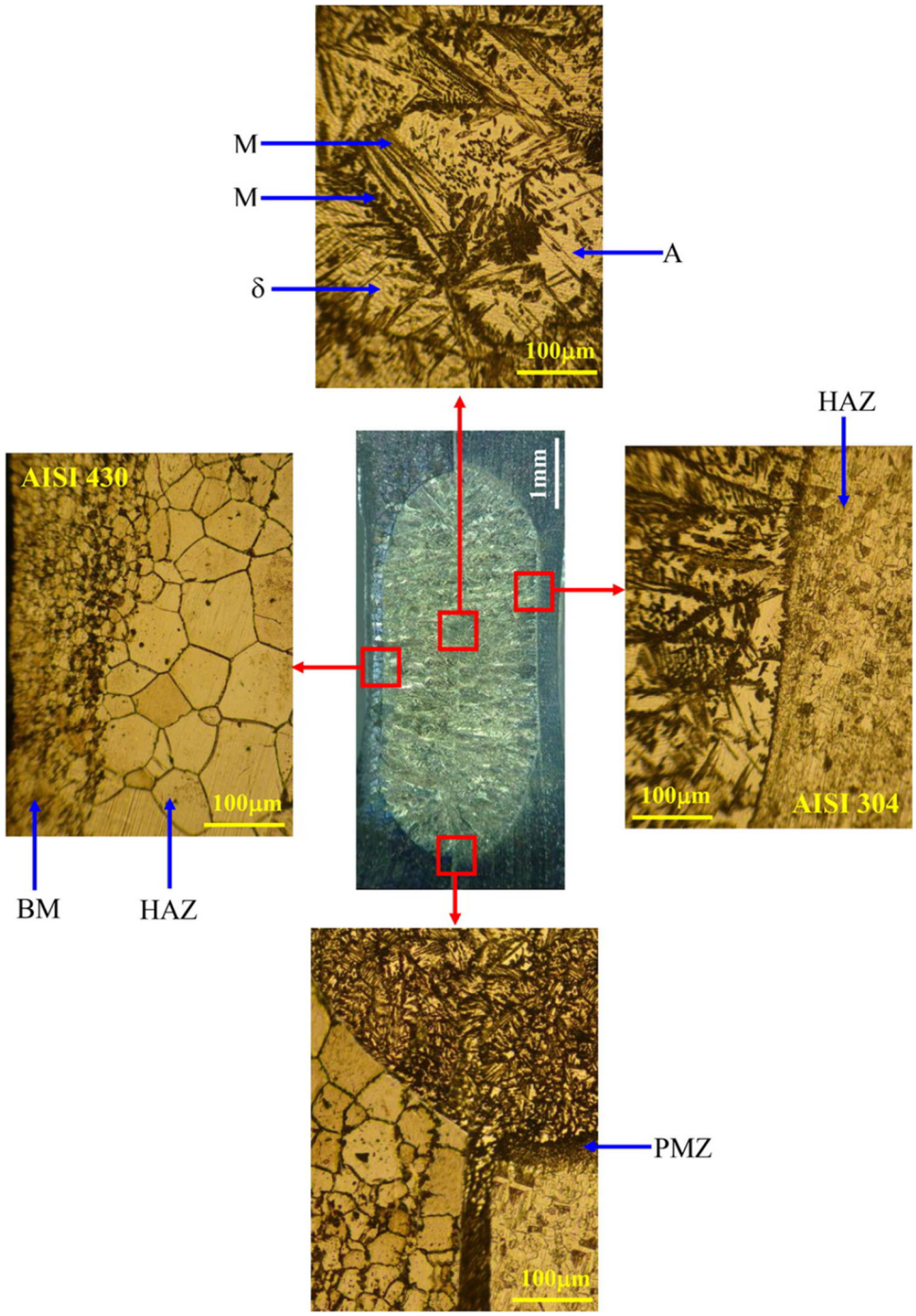

Fig. 8 Microstructure of resistance spot welded sample with 1.2 s welding time

times. As mentioned before, due to structure of austenitic and ferritic stainless steel, the microstructure of the joint does not change so, the hardness of the welded materials cannot be changed considerably. Therefore, it can be concluded that the welding time does not have an important effect on the microhardness distribution of weld joints.

In the present work, all the welded samples were tensile shear tested in order to evaluate the weld quality. Structures employing spot weld are usually designed so that the welds are loaded in shear when the parts are exposed to tension or compression loading. In some cases, the welds may be loaded in tension, where the direction of loading is normal to the plane of the joint, or a combination of tension and shear [3, 18]. Therefore, the effect of various welding times on the tensile shear strength of joined materials was evaluated and results are given graphically in Fig. 10. It was found that tensile shear load of welded samples increased with welding time. In fact, increasing the welding time caused high heat input to weld zone and extending to weld nugget, so the tensile shear strength of joints

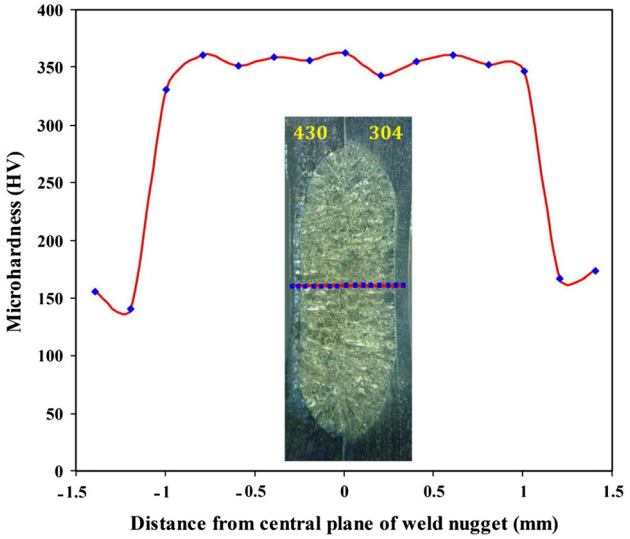

Fig. 9 Microhardness of sample with 1.2 s welding time

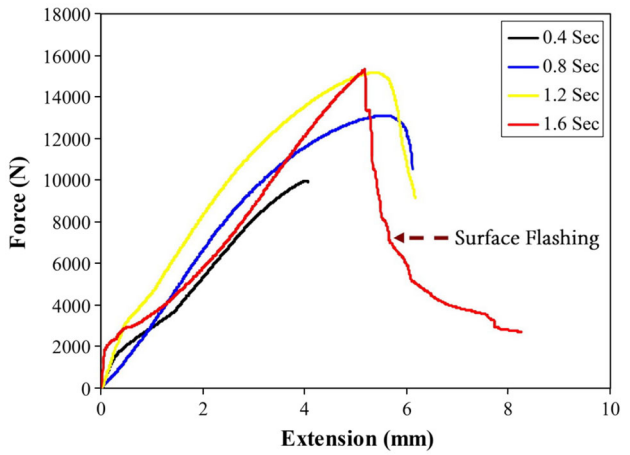

Fig. 10 Tensile shear load–extension curves of the welded samples at various times

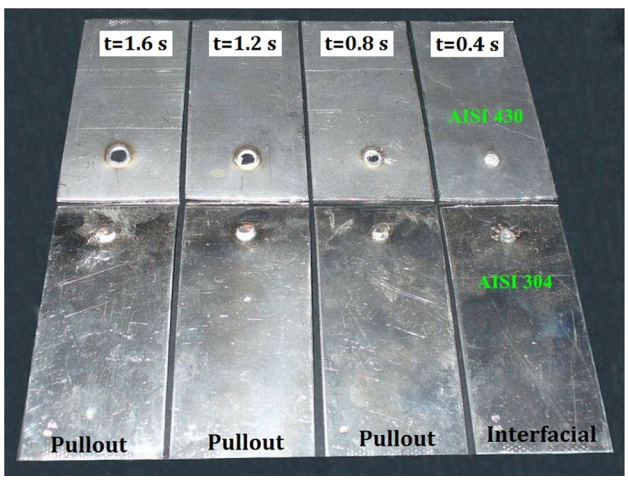

Fig. 11 Macrostructural of the fracture surface of spot welded samples for various welding times

improved. In other words, the enhancement in tensile shear load of weldment is primarily attributed to the enlargement of nugget diameter. These results are consistent with the results of the macrostructural observations. When welding time is more than 0.4 s, the tensile shear strength rapidly increases, then dwindles and finally saturates by further times. The maximum value of it was obtained in 1.2 and 1.6 s. But, for sample with maximum welding time, the overheating between the electrodes and the samples caused surface flashing, pick up of metal on the electrode, and poor surface appearance. For this reason, the shape of tensile shear load–extension curve for 1.6 s welding time wasn't similar to other samples. Therefore, it can be concluded that the optimum welding time resulting in maximum joint strength was established at 1.2 s for chosen weld current.

3.4 Failure Behavior

Figure 11 shows the effect of the welding time on the failure mode of resistance spot welded samples. As shown in Fig. 11, two distinct failure modes were observed during tensile shear testing: interfacial and pullout failure modes. The sample with minimum welding time showed a typical fracture surface of a spot welds which had failed in the interfacial failure mode. During failure, spot welded joint fails through weld nugget centerline. Other samples showed a typical fracture surface of a spot welds which had failed in the pullout failure mode. From Fig. 11, it is obvious that the failure is initiated from ferritic stainless steel side. It is generally expected that failure occurs in the softer region of the spot weld during the tensile shear test.

4 Conclusions

The investigation of welding between austenitic stainless steel (AISI 304) and ferritic stainless steel (AISI 430) by resistance spot welding process reaches the following conclusions:

1. As the welding time was increased the nugget diameter increased on both sides. However, the nugget diameter on the austenitic stainless steel side was greater than ferritic stainless steel. The reason was that austenitic stainless steel had a higher electrical resistance.
2. The microstructure of weld metal consisted of austenite, martensite, and ferrite (δ). The increase in welding time caused coarsening of the microstructure of weld nugget and also of HAZ.
3. Cavity in the centre of the weld nugget joined at maximum welding time (1.6 s) was observed. These

internal defects in spot welds are caused by high welding time.
4. Microhardness values of the welded samples were not fluctuated.
5. Tensile shear strength of the welded samples was increased with welding time.
6. The determined fracture types of welded samples were interfacial failure mode, in low welding time (0.4 s), and pullout failure mode, in higher welding time (0.8, 1.2, and 1.6 s).
7. The optimum welding time producing maximum joint strength and acceptable joint was established at 1.2 s.

References

1. Satyanarayana V V, Madhusudhan Reddy G, and Mohandas T, *J Mater Proc Technol* **160** (2005)128.
2. Reiter A E, Brunner B, Ante M, and Rechberger J, *Surf Coat Technol* **200** (2006) 5532.
3. Ozyurek D, *Mater Des* **29** (2008) 597.
4. Kwok CT, Fong S L, Cheng F T, and Man H C, *J Mater Proc Technol* **176** (2006) 168.
5. Gulenc B, Develi K, Kahraman N, and Durgutlu A, *Inter J Hyd Ener* **30** (2005) 1475.
6. Carry H B, *Modern Welding Technology*, 2nd Edition, American Welding Society, Prentice Hall (1981), p 497.
7. Lee W S, Cheng J I, and Lin C F, *Mater Sci Eng A* **381** (2004) 206.
8. Aslanlar S, *Mater Des* **27** (2006) 125.
9. Kocabekir B, Kacar R, Gunduz S, and Hayat F, *J Mater Proc Technol* **195** (2008) 327.
10. Chou Y, and Rhee S, *Weld J* (2003) 195s.
11. Sun Z, *Int J Pres Ves Piping* **68** (1996) 153.
12. Samal MK, Seidenfuss M, Roos E, and Balani K, *Eng Fail Anal* **18** (2011) 999.
13. Anawa E M, and Olabi A G, *Opt Las Eng* **46** (2008) 571.
14. Welding processes, *AWS Welding Handbook* 7th Edition, vol. 3, American Welding Society, Macmillan Press Ltd, London (1980).
15. Hasanbasoglu A, and Kacar R, *Mater Des* **28** (2007) 1794.
16. Pouranvari M, Mousavizadeh S M, Marashi S P H, Goodarzi M, and Ghorbani M, *Mater Des* **32** (2011) 1390.
17. Marashi P, Pouranvari M, Amirabdollahian S, Abedi A, and Goodarzi M, *Mater Sci Eng A* **480** (2008) 175.
18. Vural M, and Akkus A, J Mater Proc Technol (2004) 153.
19. Harlin N, and Jones T B, *J Mater Proc Technol* **143–144** (2003) 448.